NASA/TP—20220011323

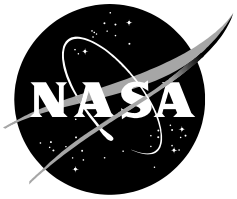

Power Surge Testing for Polymer Tantalum Capacitors

Alexander A. Teverovsky

Sept 2022

NASA STI Program Report Series

The NASA STI Program collects, organizes, provides for archiving, and disseminates NASA's STI. The NASA STI program provides access to the NTRS Registered and its public interface, the NASA Technical Reports Server, thus providing one of the largest collections of aeronautical and space science STI in the world. Results are published in both non-NASA channels and by NASA in the NASA STI Report Series, which includes the following report types:

- TECHNICAL PUBLICATION. Reports of completed research or a major significant phase of research that present the results of NASA Programs and include extensive data or theoretical analysis. Includes compilations of significant scientific and technical data and information deemed to be of continuing reference value. NASA counterpart of peer-reviewed formal professional papers but has less stringent limitations on manuscript length and extent of graphic presentations.

- TECHNICAL MEMORANDUM. Scientific and technical findings that are preliminary or of specialized interest, e.g., quick release reports, working papers, and bibliographies that contain minimal annotation. Does not contain extensive analysis.

- CONTRACTOR REPORT. Scientific and technical findings by NASA-sponsored contractors and grantees.

- CONFERENCE PUBLICATION. Collected papers from scientific and technical conferences, symposia, seminars, or other meetings sponsored or co-sponsored by NASA.

- SPECIAL PUBLICATION. Scientific, technical, or historical information from NASA programs, projects, and missions, often concerned with subjects having substantial public interest.

- TECHNICAL TRANSLATION. English-language translations of foreign scientific and technical material pertinent to NASA's mission.

Specialized services also include organizing and publishing research results, distributing specialized research announcements and feeds, providing information desk and personal search support, and enabling data exchange services.

For more information about the NASA STI program, see the following:

- Access the NASA STI program home page at http://www.sti.nasa.gov

- Help desk contact information:

https://www.sti.nasa.gov/sti-contact-form/ and select the "General" help request type.

NASA/TM—20220011323

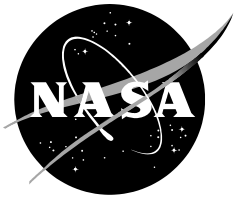

Power Surge Testing for Polymer Tantalum Capacitors

Alexander A. Teverovsky
Jacobs Engineering Group, Lanham MD

National Aeronautics and
Space Administration

Goddard Space Flight Center
Greenbelt, MD 20771

September 2022

Acknowledgments (optional)

This work was sponsored by the NASA Electronic Parts and Packaging (NEPP) Program.

Level of Review: This material has been technically reviewed by technical management.

Available from

NASA STI Program
Mail Stop 148
NASA's Langley Research Center
Hampton, VA 23681-2199

National Technical Information Service
5285 Port Royal Road
Springfield, VA 22161
703-605-6000

This report is available in electronic form at

https://nepp.nasa.gov/

ABSTRACT

Due to dry environments, anomalous charging currents (ACC) in polymer tantalum capacitors (PTC) could cause malfunctions or failures in space systems. Currently, there is no standard metric to assess this effect, and factors affecting ACC are not well understood. This paper discusses the benefits and drawbacks of different methods used to reveal ACC, and suggests power surge testing (PST) as a procedure for screening and qualification of PTCs for space applications. The suggested test is similar to the surge current testing that is currently used for MnO2 tantalum capacitors but assures dissipation of high power in the part throughout testing. Using various types of capacitors, the reproducibility of test results for different manufacturing lots of PTCs and from sample to sample within a lot were estimated. The impact of moisture content, test temperature, stress voltages, and preconditioning were assessed. Thermal effects associated with ACC and the possibility of catastrophic failures were studied experimentally using an IR camera and calculated at adiabatic heating conditions. Possible mechanisms of the phenomenon are discussed and recommendations for testing to avoid failures related to ACC are suggested.

I. INTRODUCTION

A peculiarity of polymer tantalum capacitors (PTC) that is not observed in MnO2 capacitors (MTC) is the presence of anomalous transients. These transients include a group of phenomena that happens after application of voltage pulses to initially discharge and dry capacitors. The phenomena is revealed as increased capacitance, dissipation factor, and leakage currents that (contrary to MTC) are voltage dependent and can rise at lower temperatures [1]. High levels of leakage currents that are especially significant within the first several or dozens of milliseconds after voltage application was first discovered by Y. Freeman and co-workers, and named them anomalous charging currents (ACC) [2]. The level of ACC can exceed 1 A and cause temporary shorts and malfunctions in some electronic systems. ACC might also increase substantially the time that is necessary to charge capacitors that is not acceptable for fast-acting circuits e.g., power supplies in solid state drives (SSD).

Application of a step rated voltage (VR) to a capacitor of value C results in displacement currents, I_{disp}, that reduce with time exponentially with the characteristic time $\tau = C \times ESR$, where ESR is the equivalent series resistance of the part. For capacitors in the range from 10 to 470 μF, VR from 10 to 50 V, and ESR below 0.1 ohm, the amplitude of the displacement current transient exceeds 100 to 500 A with the width of the spike, τ, below 47 μsec. Due to fast relaxation, displacement currents in most capacitors become negligibly small after 1 msec. Absorption currents that are typically below a few milliamperes decrease inversely with time, and determine leakage currents in capacitors from tens to thousands of seconds [3]. Afterwards, the currents stabilize at levels that correspond to the intrinsic leakage of the dielectric and may be orders of magnitude below the specified direct current leakage (DCL).

Displacement currents are caused by changes in the electric field of the dielectric with time. Absorption currents are due to reorientation of dipoles or electron trapping into states within the dielectric or at the interface cathode/dielectric. Leakage currents are related to the intrinsic conductivity of the dielectric. The first two types increase linearly with voltage and have poor temperature dependence, whereas the leakage current increases exponentially with temperature and voltage.

All three types of the currents are present in both MnO2 and polymer tantalum capacitors. However, only PTCs have the additional characteristic, ACC. Although the nature of ACC is not clearly understood, it is most likely related to the Schottky emission of charge carriers over the barrier at the conductive polymer/T2O5 dielectric interface. Rising of the barrier with time that results in the current relaxation was explained by the orientation of polymer dipoles in [2, 4] or by electron trapping processes and specifics of the electronic state structure of conductive polymers in [1].

Since first discovered in 2013, all investigations of ACC [5-7] confirm that the phenomenon is specific to dry PTCs only, with the level of ACC increasing with voltage and decreasing at high temperatures but increasing at low temperatures. Development of new, modified conductive polymers, and improvements of the technology and processes of the oxide formation may suppress anomalies transients substantially [4, 8].

The lack of information about factors affecting ACC and means to control its level during manufacturing are mostly due to the absence of a standard technique to characterize the effect. The purpose of this work is to analyze possible test methods, suggest power surge testing (PST), and to assess various factors affecting results of PST that include voltage, temperature, preconditioning and the moisture variation level during bake and reflow soldering.

II. TECHNIQUES

To analyze ACC, variations of currents and voltages should be monitored in the process of charging. These variations depend on the dynamic characteristics of the power supply and the set-up conditions. Three methods of charging can be used: constant voltage ramp (CVR), constant current (CC), and constant voltage charging. The CVR was used at a ramp rate of 120 V/sec in several publications [5-7, 9]. The level of ACC at the rated voltage during CVR testing depended on the ramp rate and type of capacitors. To compare test results for different types of capacitors, the currents should be normalized to the value of the capacitance. Variations of the normalized values of I_{ACC} and I_{displ} with the ramp rate are shown in Fig.1. Depending on the part type, I_{ACC} varies with the ramp faster or slower than I_{displ}. - In general, there is no optimal rate to get maximum ratio of I_{ACC} and I_{displ}.

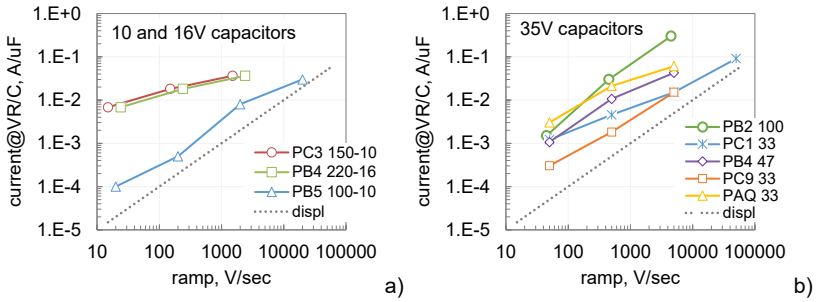

Fig.1. Variations of displacement and charging currents normalized to capacitance with the ramp rate for different 10 and 16 V (a) and 35 V (b) capacitors. The currents in amperes are normalized to the value of capacitance in μF.

2.1. Power surge testing

During PST, the part is stressed by a voltage pulse with the amplitude corresponding to the rated voltage while the current is recorded with time, typically up to 100 msec. Because ACC occurs right after the displacement current transient with a duration typically less than 1 msec, the power supply should be capable of stabilizing voltage within 1 msec. In this study, the advanced high-speed dynamic sourcing and measurement power system, N7973A, from Keysight was used to generate 200 msec power on/off cycles at currents limited from 0.3A up to 30 A and voltages up to 60 V. This power supply can stabilize voltage within 0.3 msec even at currents of more than 30 A.

The PST is similar to the surge current testing (SCT) that is currently used to assure that MTCs are capable of withstanding high displacement currents and have instant breakdown voltages above VR. To create high surge current, a large bank capacitor (more than 20 times the value of the DUT) pre-charged to VR is discharged onto the tested capacitor. This creates a current spike with an amplitude $VR/(R+ESR)$, where R is the resistance of the connecting circuits. If due to ACC, the current through the part remains large, the bank capacitor will discharge so the level of the stress will decrease substantially. At these conditions the actual duration of the stress during SCT does not exceed ~ 1 msec.

Contrary to SCT, the level of voltage stress and the power dissipated within the part remains high during the whole period of PST. Examples of PST for different part types and manufacturing lots of capacitors are shown in Fig.2. In some cases, at relatively low levels of ACC the currents decrease with time according to the power law, $I \sim t^{-n}$ with the constant n close to 1, which is similar to the behavior of absorption currents. Fig. 2b gives an example of PST results when the power supply limits currents at a 3 A level. At relatively large levels of ACC, current relaxation curves might have humps as shown in Fig.2c. Results shown in Fig.2 indicate a substantial spread of data within each lot and from lot-to-lot. Similar large spread of ACC levels was also reported in [6, 7] and confirms the need to control ACC during manufacturing.

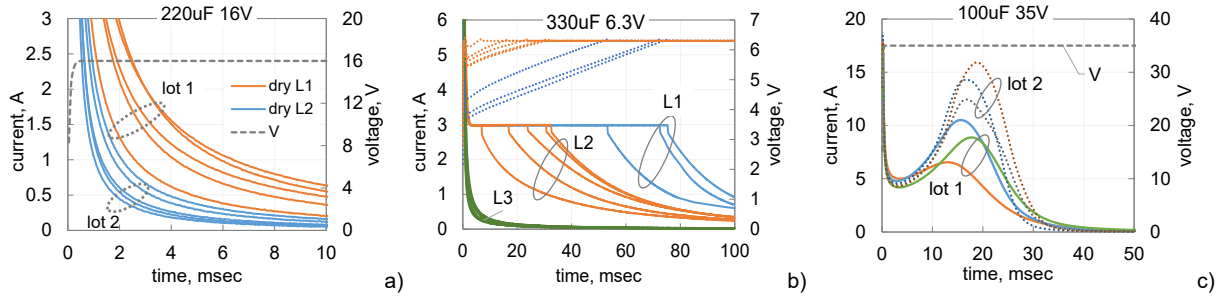

Fig.2. Results of PST for two lots of 220 µF, 16 V (a), three lots of 330 µF, 6.3 V (b), and two lots of 100 µF 35V (c) polymer tantalum capacitors. Different curves correspond to different samples in the lot. Solid lines in (b) correspond to current and dotted lines to voltage variations.

Energy dissipated in the process of anomalous transients was calculated by digital integration of the recorded currents and voltages, $Q = \Sigma(I \times V \times \Delta t)$. For PST, the integration was carried out up to the moment when the current decreased to below 0.01 A, and for the CVR technique to the moment when the voltage reached VR.

The value of energy dissipated during PST gives an assessment of ACC that does not depend on the specifics of current relaxation. However, to simplify characterization of the test results, average and standard deviations of currents measured after 10 msec after pulse application, I_{10}, for a group of 5 to 10 samples can be used. The coefficients of sample-to-sample variations within one lot are typically in the range from 5 to 50%, and the values of I_{10} for different lots of capacitors might vary from 0.01 A to more than 10 A. Variations of Q are smaller than I_{10} and are relatively independent on the value of limiting currents. Based on I_{10}, the severity of ACC can be characterized as high for parts with $I_{10} \geq 1$ A, as low for parts with $I_{10} < 0.1$ A, and as medium for $0.1 \leq I_{10} < 1$ A.

Results of the energy calculations for capacitors shown in Fig.2 are displayed in Table 1. In all cases, despite a relatively large spread of the data (the coefficient of variance was in the range from 9 to 29%) there is a statistically significant difference in the values of Q for different lots of the same part types. Also, the accuracy of ACC assessments using values of Q for lots with relatively large currents is better compared to I_{10}. For example, for 8 samples of 33 µF 35 V dry capacitors the average I_{10} was 2.17 A at a standard deviation of 0.41 A, whereas these values for Q were 2.58 J and 0.22 J. This data corresponds to the coefficients of variations of 19% for I_{10} and 8.4% for Q.

Calculations of the dissipated energy for CVR testing were made at different voltage ramp rates. Results of these calculations for six types of capacitors are shown in Fig.3. In all cases, the dissipated energy decreased with the ramp rate, and as expected was substantially (at least two times) less than during PST.

Table 1. Average/standard deviation values of the dissipated energy Q in J for 220 µF 16 V, 330 µF 6.3 V, and 100 µF 35 V capacitors shown in Fig.2.

lot	220-16	330-6	100-35
L1	0.42/0.12	1.32/0.14	6.4/0.75
L2	0.15/0.04	0.91/0.19	8.6/0.82
L3		0.11/0.02	

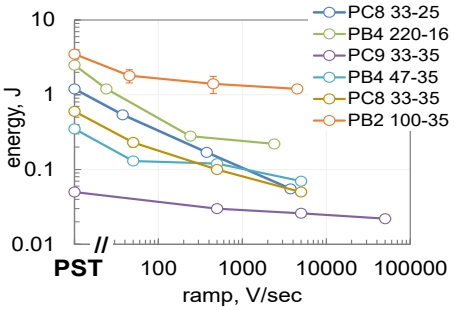

Fig.3. Variations of energy dissipated during ACC testing using the CVR method at different ramp rates and during PST for six types of capacitors. For comparison, the values of energy corresponding to PST are shown on the same chart as for CVR tests.

Based on results of previous studies carried out using the CVR method [6, 7], no failures were observed even for samples with high levels of ACC. However, PST did reveal failures in capacitors. The propensity to failure is lot-related and increases after reflow soldering simulations. In one of the lots, up to 20% of the parts failed PST after a month of storage at 85 °C. Examples of PST failures are shown in Fig.4. The time to failure varied from a few

milliseconds up to more than 80 msec in some cases. Similar to surge current testing of MnO2 capacitors [10], PST failures might happen after a few test cycles as shown in (see Fig 4c) for a 100 µF 35 V capacitor tested at -55 °C.

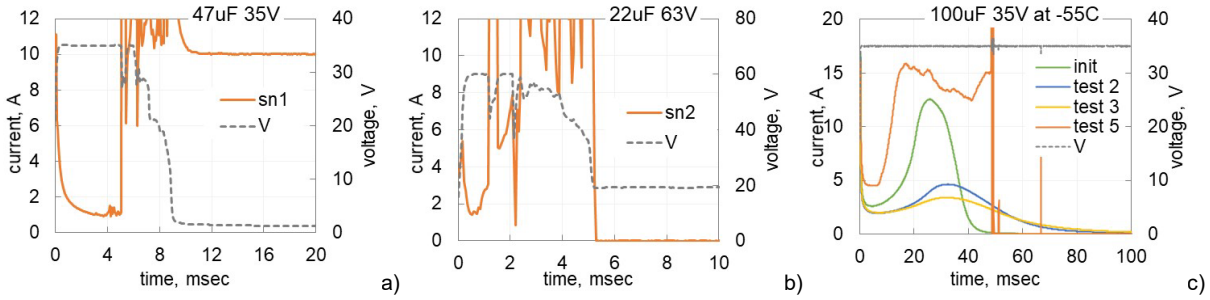

Fig. 4. Failures during power surge testing in different part types at room conditions (a, b) and at -55 °C (c).

III. FACTORS AFFECTING ACC

Factors affecting ACC that were analyzed in this study include the number of test cycles, preconditioning, temperature, bake conditions, voltage, and soldering reflow.

3.1. Repeat testing

Displacement and absorption currents in tantalum capacitors restore to their initial values during repeat testing following depolarization. Contrary to that, anomalous transient currents are decreasing with the number of test cycles that include equal periods of polarization and depolarization. As an example, Fig.5 shows results of several consecutive tests using CVR and PST techniques. The level of ACC decreases with each consecutive test and typically takes ~ 30 sec to record the data and reset the tester. To restore the initial level of ACC, baking the components for several days at 85 °C or a few hours at 125 °C is required.

Results of the CVR studies in [6, 7] showed that ACC decreases with repeated on/off cycles. In our tests, the trend of ACC reduction during consecutive tests was found in all part types. However, the degree of the current decrease appears to be greater for parts with initially higher charging currents (see Fig.4b). Repeat testing results in a significant, up to 5 times, reduction of the currents compared to the initial test. After that, additional cycles continue suppressing ACC, but less effectively.

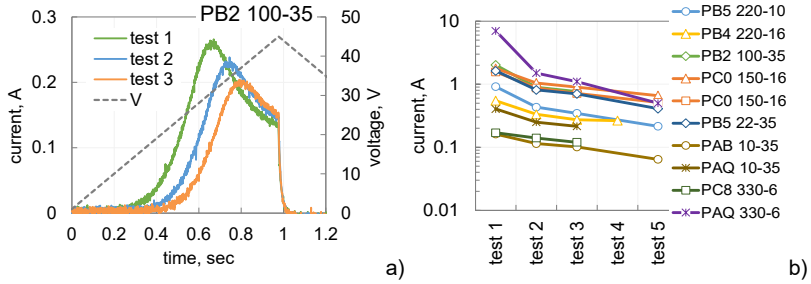

Fig.5. Results of CVR (a) and PST (b) for several consecutive tests using the same samples. Fig.(b) shows variations of currents measured after 10 msec of PST for various types of capacitors.

3.2. Preconditioning.

All previous studies indicated that moisture absorbed in capacitors suppresses the level of ACC substantially. However, the effect of the amount of moisture has not been studied. In this work, a relative amount of moisture in the parts was assessed by measurements of capacitance, as was suggested in [11]. To saturate the parts with moisture, they were stored in a humidity chamber at 85 °C and 85% RH for one week. To dry out the parts, they were baked for at least 16 hours at 125 °C. Respectively, depending on the preconditioning of the capacitors, they were called wet or dry.

To evaluate the sensitivity of ACC to moisture content, two lots of 100 µF 35 V polymer capacitors were tested initially in the as-received state, after moisturizing, baking, and then with time of storage at room conditions (20 °C and 40% RH) for four weeks. Results of these measurements are shown in Fig.6. Moisturizing resulted in

approximately a 10% increase of capacitance and a decrease of current by more than 2 orders of magnitude compared to the as-received condition. Baking restored capacitance to the initial value for lot 1 and decreased it by ~10% for lot 2, which might be due to different initial levels of moisture. Drying increased the currents in both lots above the level in the as-received condition. Storing at room conditions for four weeks reduced currents to the level of wet capacitors, whereas capacitance stabilized at the levels well below the level of wet parts.

Assessments based on capacitance measurements indicate that the level of moisture after storing at room conditions corresponds to 50% to 60% of the level for wet capacitors. Note, that 3 to 7 times reduction of current occurred after 3 hours at room conditions. This reduction is substantially greater than what might be caused by repeat testing, so the effect was mostly due to the moisture uptake. These data indicate that even a relatively small amount of moisture, less than 10% of the amount absorbed at room condition, can has a significant effect on ACC. For this reason, it is critical to specify that the PST measurements should be taken within, but not more than 3 hours after the bake.

To illustrate the sensitivity of ACC to bake conditions, three types of PB5 capacitors were tested after a 3-hour bake at 150 °C and a 168-hour bake at 125 °C. Fig. 6c shows that after the 150 °C bake I_{10} currents increased by an order of magnitude compared to the initial level. However, additional bake at 125 °C for 168 hours increased currents by almost two orders of magnitude.

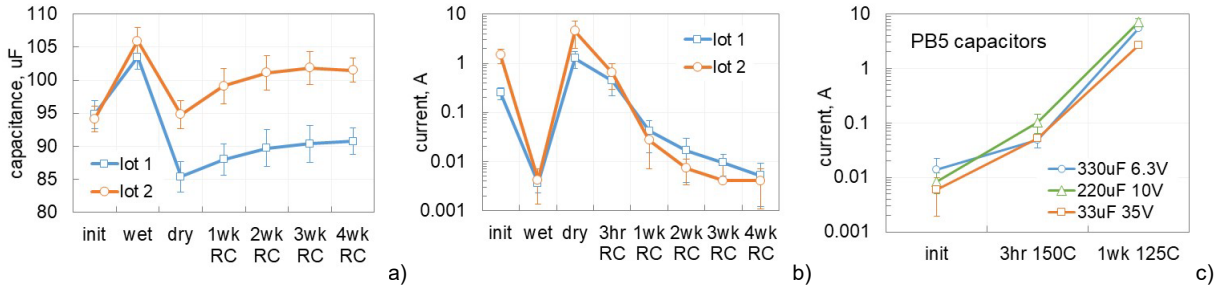

Fig.6. Variations of capacitance (a) and currents measured at 10 msec of PST (b, c) in the process of preconditioning and storage at room conditions. Figure (c) shows currents in three types of PB5 capacitors after different bake conditions.

To assess the effect of bake duration at different temperatures, PST was carried out on five types of PTCs during baking first at 85 °C for 4 weeks, then at 125 °C for four hours, and finally for 1 week more at 125 °C. Capacitance was also monitored to assess variations in the moisture content. Results of these tests are shown in Fig.7. The level of ACC increases substantially after the first week at 85 °C, on average by 7 times. Afterwards, ACC remained stable with increases by 20 to 30% only during 3 more weeks of storage. Four hours at 125 °C did not change capacitance and currents significantly, but they increased from 3.5 to more than 30 times for different part types after one week at 125 °C.

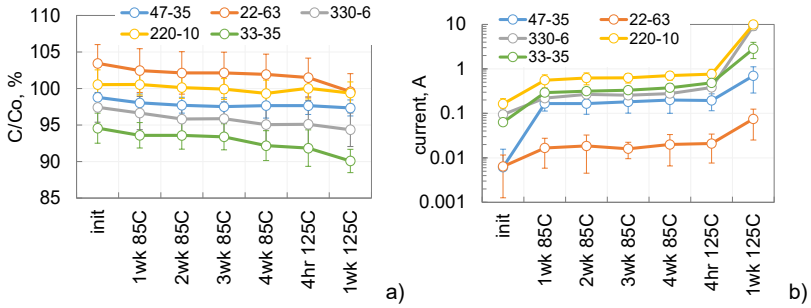

Fig.7. Variations of capacitance (a) and currents measured at 10 msec of PST (b) for five types of polymer capacitors during a 4 week bake at 85 °C followed by 1 week bake at 125 °C.

Based on results presented in Fig.7a, relative variations of the moisture content in the parts compared to the amount of moisture in wet capacitors (after one week at 85 °C and 85% RH) were calculated as:

$$\Delta m = 100\,\frac{C - C_{dry}}{C_{wet} - C_{dry}}, \qquad (1)$$

In the as-received condition, the parts were initially relatively dry, with the moisture content varying from 7 to 35% (17.5% on average) of the amount of moisture in wet parts. After one week of bake at 85 °C, the amount of moisture

decreased on average to 12.5%, and decreased further to 7.6% after four weeks. Additional bake at 125 C for 4 hours reduced Δm to 6.9% of the amount absorbed in wet parts. Although there is a clear trend for capacitance reduction and an increase of ACC caused by increased duration or bake temperature, no direct correlation between changes of these two characteristics was found. Moreover, a relatively small decrease in capacitance after one week at 125 °C compared to the 4-hour bake that resulted in reduction of Δm likely below 5%, caused a 3.5 to 24 times increase in ACC currents. Results show that ACC currents are much more sensitive to moisture compared to capacitance.

3.3. Temperature

Transient currents measured during PST in three types of capacitors at temperatures from -55 to +125 °C are shown in Fig.8. In all cases, variations of temperature changed not only the level of currents, but also the rate of relaxation. At temperatures above 20 °C, the currents after a few milliseconds were relaxing much faster than at lower temperatures. In double logarithmic coordinates, portions of *I-t* curves can be approximated with straight lines, so variations of currents with time can be described using the power law, $I \sim t^{-n}$. For 150 µF 16 V capacitors shown in Fig.8b the values of *n* are 2.1 and 0.3 at 105 °C and -40 °C respectively. Currents in 330 µF 6.3 V capacitors at -55 °C (Fig.8c) have a hump with maximum current reaching 10 A at 20 msec. At higher temperatures the maximum decreases, occurs earlier, and practically disappears at T > -25 °C.

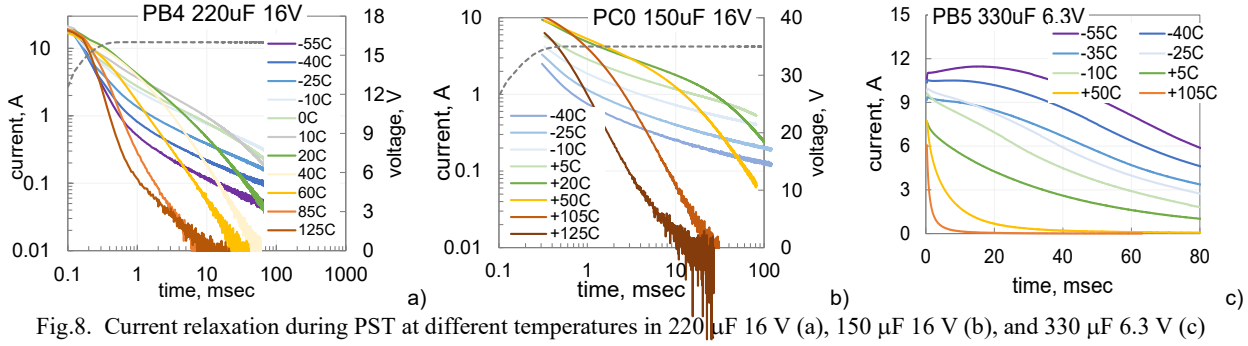

Fig.8. Current relaxation during PST at different temperatures in 220 µF 16 V (a), 150 µF 16 V (b), and 330 µF 6.3 V (c) polymer capacitors.

Variations of I_{10} with temperature in the range from -55 °C to +125 °C for different types of capacitors are shown in Fig.9. To avoid reduction of currents caused by repeat measurements, different groups of capacitors (3 to 5 samples in a group) were used for the testing at each temperature. In most cases, $I_{10}(T)$ curves had maximum that depending on the part type varied between -55 °C and +30 °C. The maximum current, I_{max}, was in the range from 10 A down to a few milliamperes. At temperatures below or above T_{max}, the currents decreased significantly from several times to orders of magnitude. In most cases, the currents at 125 °C were close to or below 0.01 A.

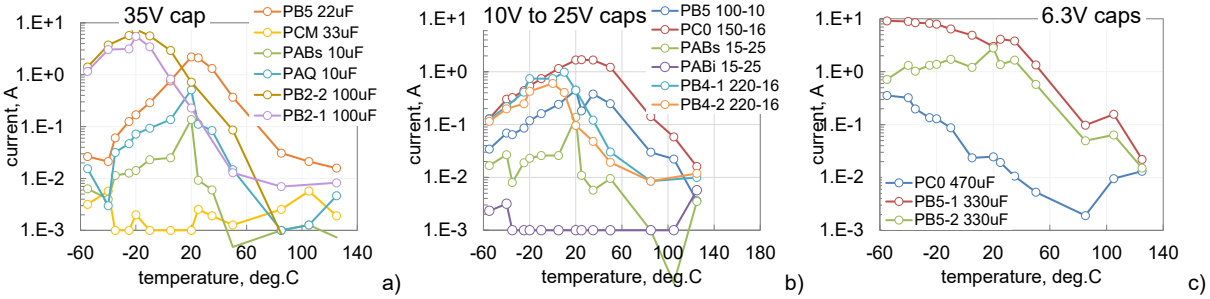

Fig.9. Temperature variations of currents measured at 10 msec of PST for different types of polymer tantalum capacitors rated to 35 V (a), 10 and 25 V (b), and 6.3V (c).

Based on results of previous studies [2, 6], a greater level of ACC was expected for higher voltage capacitors that are manufactured using pre-polymerized PEDOT:PSS compositions. The low-voltage parts that use in-situ polymerization of PEDOT polymers had substantially lower levels of ACC. It was also observed that the level of ACC increases at lower temperatures [2, 5, 6], but according to our data, there is no correlation between the rating of the parts and the values of T_{max} or I_{max}. Additionally, some 6.3 V capacitors had $I_{max} \approx 10$ A, which is greater than the maximum level observed in parts rated to higher voltages.

Results of PST at different temperatures for two types of capacitors that had humps on *I-t* curves are shown in Fig.10. In both cases, reduction of temperature increased the time for reaching maximum hump currents. The humps at -20 °C are not clearly separated and appear to increase the rate of relaxation. For 22 µF 35 V capacitors (Fig.10b), the position of the hump changes from 5 msec at +35 °C to more than 100 msec at -20 °C, and the amplitude decreases from 4 A at +35 °C to 1.4 A at -10 °C. Temperature dependence of the time corresponding to the hump maximum is shown in Fig.10c and indicates an activation energy of 0.4 eV.

The humps on *I-t* curved during PST can be explained by the space charge limited transient currents theory developed by Many and Rakavy [12]. According to this theory, a space charge front of injected carriers moves through the dielectric resulting in maximum current when it reaches the opposite electrode. The time to the current peak, t_p, depends on the mobility of carriers, μ, applied voltage, V, and for a dielectric of thickness d can be calculated as

$$t_p = {0.787d^2}/{\mu V}\,, \qquad (2)$$

In our case, assessments based on Eq.(2) yielded $\mu \sim$ 1E-13 m^2/V-s. This theory was also used by Aris and Lewis [13] to explain maximums on transient currents in Ta2O5 dielectrics under reverse polarity, when tantalum is negative. According to their assessments the mobility was below 1E-15 m^2/V-s. Although the activation energy of currents was also ~ 0.4 eV, the mobility of the carriers was orders of magnitude lower compared to our data. Similar values of E_a = 0.4 eV and μ = 5E-14 m^2/V-s for conductivity of Ta2O5 dielectrics formed by the chemical vapor deposition were reported in [14] and explained by the protonic conduction in the dielectric. More analysis is necessary to explain the mechanism of conduction in PTCs during anomalous transients.

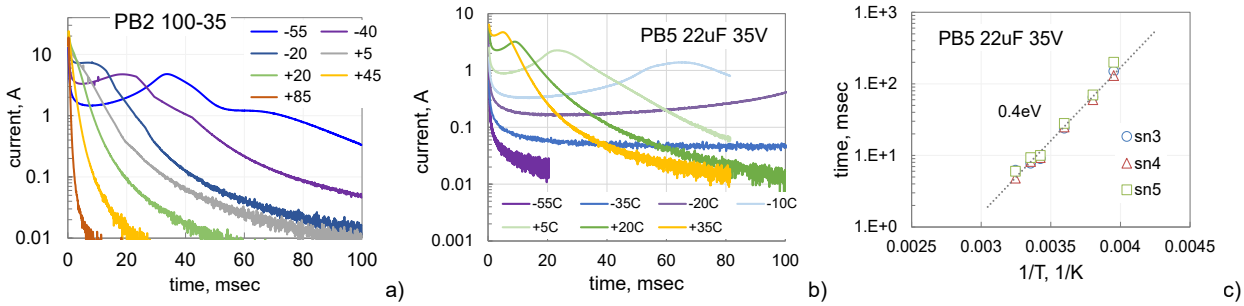

Fig.10. Current relaxations in 100 µF 35 V (a) and 22 µF 35 V (b) capacitors during PST at different temperatures and temperature variations of the time corresponding to the maximum hump current for three samples (c).

3.4. Voltage

As was expected, and based on previous studies [2, 6, 7], the test voltage had a strong effect on the level of ACC. According to PST data presented in Fig.11, the rising voltages not only increase currents substantially, but also affect the shape of *I-t* curves. The time to reach maximum hump current for parts shown in Fig.11a decreased from 65 msec at 30 V to 5 msec at 40 V. Qualitatively, this behavior is consistent with the space charge limited transient current model. However, according to Eq.(2) the time should be inversely proportional to voltage, whereas experimental data indicate a much faster variation of t_p.

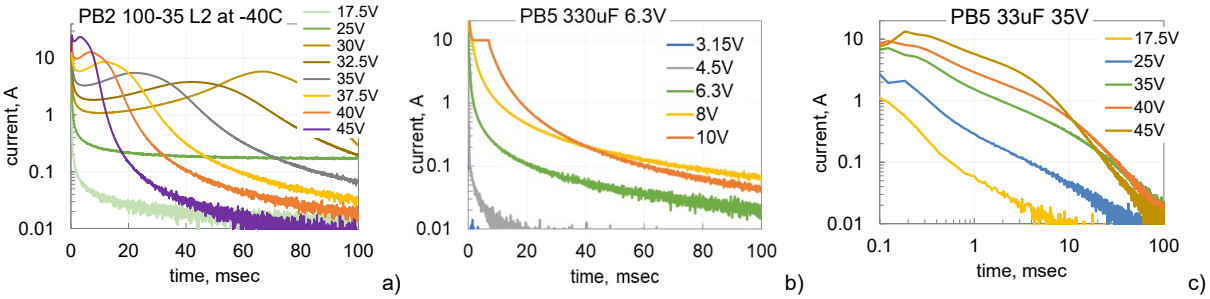

Fig.11. Results of PST at different voltages for six types of capacitors.

Variations of 10 msec currents with applied voltage for different types of capacitors are shown in Fig.12. At relatively low voltages corresponding to $I_{10} < 1$ A, the currents increase exponentially with the square root of voltage, which is consistent with the Schottky conduction mechanism:

$$\ln(I) \sim \frac{\beta_s}{kT} E^{0.5}, \tag{3}$$

where k is the Boltzmann's constant, β_s is the Schottky constant, $\beta_s = \left(q^3 / 4\pi\varepsilon\varepsilon_0\right)$, E is the electric field, $E = V/d$, and d is the thickness of the dielectric, $d \approx 5 \times VR$ nm.

Calculations show that slopes of the *I-V* curves in Schottky coordinates, are close to the theoretical values. This mechanism can describe behavior of currents measured at room (Fig.12a, b) and low temperatures (Fig.12c.) Deviation from the Schottky model occurs at relatively large currents exceeding 1 A (see Fig.12b) and might indicate changes in the mechanism of the conductivity.

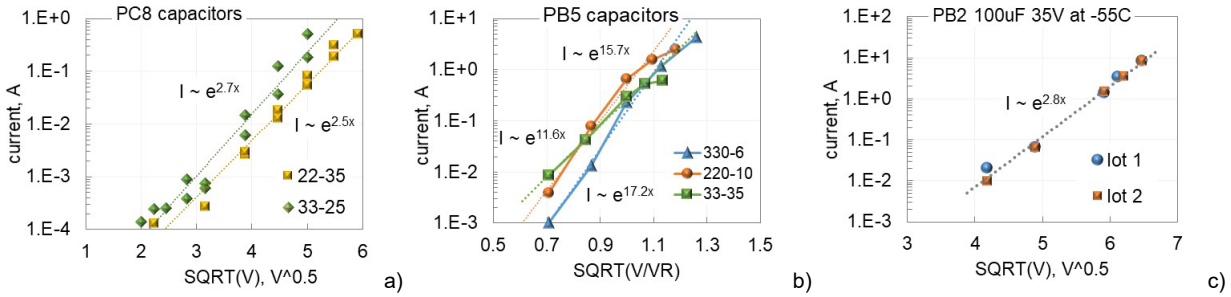

Fig.12. *I-V* characteristics measured at room temperature based on 10 msec currents for 22 µF 35 V and 33 µF 25 V (a), 330 µF 6.3 V, 220 µF 10 V, and 33 µF 35 V (b) capacitors. Note that Fig.(b) shows characteristics with voltages normalized to the rated voltage. Figure (c) shows *I-V* characteristics for 100 µF 35 V capacitors at -55 °C.

3.5. Reflow soldering.

Increasing ACC after reflow soldering had been previously reported [4] and is expected considering the reduction in moisture after exposure to higher temperatures. Analysis shows that even at relatively low temperatures used for Sn/Pb eutectic reflow soldering (235 °C), this process reduces moisture content in capacitors by 50% to 75% [15]. However, there is still a lack of information about the effect of preconditioning before soldering and the level of ACC increase after different soldering conditions.

To assess the effect of soldering, PST was carried out for several part types. Five samples were selected for before and after reflow soldering simulation with the eutectic and lead-free soldering at conditions close to those specified in J-STD-020: preheating for 100 sec at 150 °C or 200 °C and exposure to 235 °C or 260 °C for 20 sec. The parts were preconditioned either by bake at 125 °C for 20 hours (dry capacitors) or by storage for one week in a humidity chamber at 85 °C 85%RH (wet capacitors).

Different lots of the same type of dry 220 µF 16 V capacitors not only had different levels of ACC initially, but also different responses to reflow at 235 °C (Fig.13). Increasing the number of reflow cycles to three increases ACC for the initial dry capacitors but the effect is more significant for wet parts. After three reflow cycles, the initially wet capacitors had currents 2.6 times higher for lot 1 and 4 times higher for lot 2 than the post-reflow currents in the initially dry parts. Note, the most significant changes in capacitance occurred with the initially wet parts after the first reflow, whereas after the third cycle capacitance remained the same. There were no significant changes in C/C_0 for dry capacitors after the first and third reflow cycles. This confirms that the sensitivity of ACC to moisture is much greater compared to capacitance.

Temperature dependencies of PST current for two lots of 100 µF 35 V capacitors are shown in Fig.13b. Two groups of samples from each lot were preconditioned to form a set of wet capacitors and wet capacitors after reflow simulation at 235 °C. Currents in wet parts remained low at -55 °C. However, currents in capacitors after reflow soldering not only increased by approximately three orders of magnitude, but in the temperature range from +20 to -40 °C were ~2 times greater than for dry capacitors (compare with data in Fig.9a). A substantial increase of failures caused by reflow soldering of initially wet polymer tantalum capacitors compared to soldering of dry parts was also observed in [16]. One of the reasons for these failures may be a significant increase in the dissipated energy during the first power-on cycle caused by a high level of ACC.

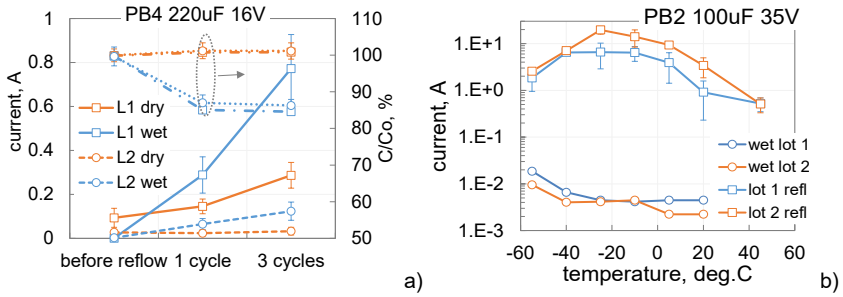

Fig.13. Variations of 10 msec PST currents and relative variations of capacitance for two lots of 220 µF 16 V capacitors before and after one and three reflow cycles (a) and temperature variations of the I_{10} currents for wet 100 µF 35 V capacitors before and after one cycle of reflow simulation at 235 °C (b).

Comparison of 10 msec PST currents for different types of wet and dry capacitors before and after reflow soldering simulations at 235 °C is shown in Fig.14. Like in the previous case, reflow of the initially wet capacitors resulted in higher currents compared to the initially dry parts for 6 lots. For three types of capacitors, 330 µF 6.3 V, 220 µF 10 V and 33 µF 35 V (Fig.14b), currents for the initially dry parts were greater than for initially wet capacitors. For one part type shown in Fig.14c, reflowing of wet parts resulted in a relatively small increase of currents, whereas post soldering currents in dry capacitors were lower than before.

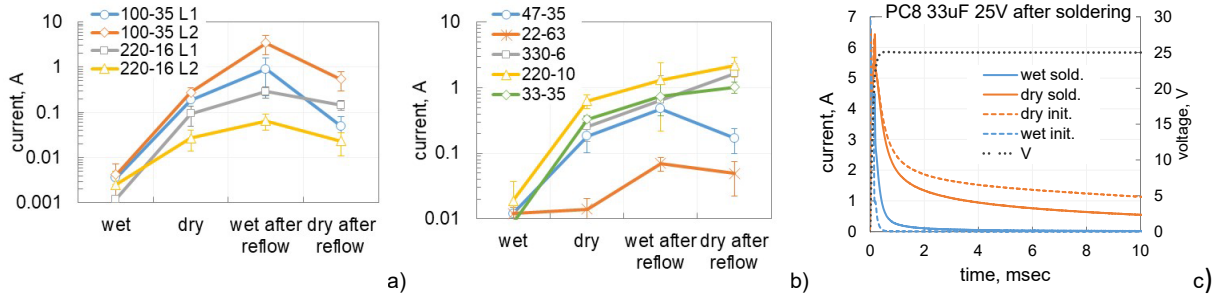

Fig.14. Effect of preconditioning on post-reflow ACC in different part types. Two lots of 100 µF 35V and 220 µF 16 V capacitors (a), five types of capacitors same as shown in Fig.3.4 (b), relaxation of currents during PST for 33 µF 25 V capacitors (c).

One reason for the difference in the effect of preconditioning on post-reflow ACC might be the difference in the levels of drying caused by soldering. Another possibility is that the exposure to high temperatures results in structural changes in the polymer cathode that depend on the moisture content. The resulting variations in the barrier height at the interface may likely be a major reason for increased ACC.

The effect of exposure to high temperatures was assessed using 2 lots of 100 µF 35 V, one lot of 47 µF 35 V, and one lot of 22 µF 63 V capacitors (see Fig.15). One subgroup of each type (5 samples) was consequently baked at 150 °C for 3 hours, 125 °C for 1 week, reflow simulation at 235 °C and 260 °C, 48 hours bake at 125 °C, and finally one week at 85 °C. Another subgroup of 5 samples, was baked at 175 °C for 4 hours instead of solder reflow simulations. The sequence of high-temperature exposure was somewhat different for 22 µF 63 V capacitors as shown in Fig.15c and f.

Variations of capacitance through testing were measured to assess relative levels of moisture in the parts using Eq.(1). The dissipated energy, Q, was calculated based on PST data as described above. Results of these tests indicate that although a 3-hour bake at 150 °C reduced the amount of moisture compared to the initial level by a factor of 2, the increase of Q was relatively small. However, the dissipated energy increased ~10 times after additional bake for 1 week at 125 °C that reduced the effective moisture content in the parts to below 1%. Surprisingly, reflow simulations of dry capacitors at 235 and 260 °C reduced Q and increased the effective moisture content for 100 µF 35V and 47 µF 35 capacitors. For these parts, a 4-hour bake at 175 °C that also slightly increased the effective moisture content, did not cause significant changes in the dissipated energy compared to the level after 1 week bake at 125 °C. Additional 48-hour bake at 125 °C of the apparently completely dry parts in both groups further increased the level of ACC but decreased it after one week storage at 85 °C.

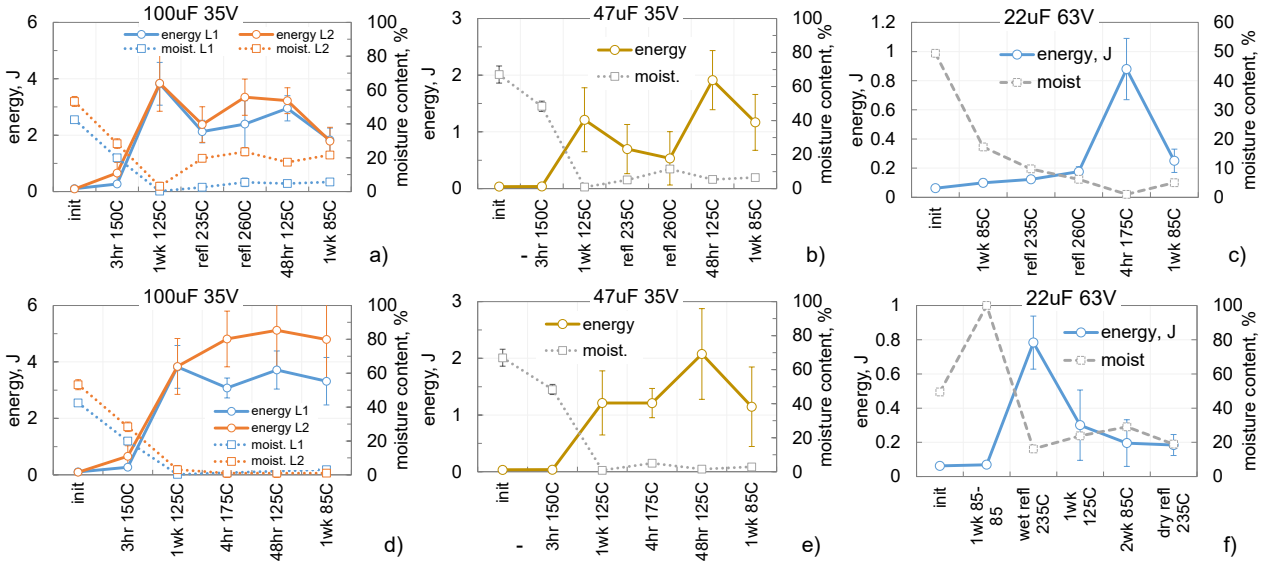

Fig.15. Variations of the dissipated energy and effective moisture content in two lots of 100 µF 35V (a, d), a lot of 47 µF 35 V (b, e) and 22 µF 63 V (c, f) capacitors during consecutive cycles of exposure to high temperatures.

Testing results of the 22 µF 63 V capacitors were qualitatively similar to the 35 V capacitors. Reflow soldering of dry parts at 235 and 260 °C (Fig. 15c) did not result in a substantial increase of ACC, whereas exposure to a 4-hour bake at 175 °C increased the dissipated energy almost 5 times. Additional bake for two weeks at 85 °C caused decrease of Q in ~4 times. The moisture content after reflow soldering simulations at 235 °C for the initially wet and dry parts were close. However, similar to results shown in Fig.13 and 14, exposure to reflow soldering temperatures resulted in a much greater dissipated energy in wet compared to dry capacitors. Possible reasons for this will be discussed in section V.

IV. THERMAL EFFECT OF ACC

To assess the thermal effect associated with ACC, temperature of the capacitors soldered onto a test PWB was monitored during PST using a FLIR infra-red (IR) camera, model A8581, at a frame rate of 30 Hz. Results of the monitoring allowed for analysis of the distributions of temperature along the surface of the part and variations of the maximum temperature with time. A reduction of temperature after the PST pulse was approximated with an exponential function that allows for the assessments of the characteristic time of temperature relaxation, τ_T.

Results of combined PST and IR camera measurements for 100 µF 35 V capacitors are shown in Fig.16. Note, that the part had dual anode slugs placed side by side, and in addition to variations of the maximal temperature with time, distributions of temperature along the slugs were analyzed as shown in the inset to figure (b). After reaching maximum temperature at the middle of the slug, in approximately 0.5 sec, the temperature reduces with $\tau_T = 5$ sec.

Analysis of the IR images show that the initial distribution of temperature along the slugs had two humps corresponding to the edges of the slug as shown in figures (c). This is due to a high density of transient currents collected by the polymer cathode at the shell area of the slug that resulted in increased Joule heating. By the time the temperature increases to maximum, after ~1 sec, the humps disappear and temperature distributions along the slug become more even. In some cases, there was a difference in the humps' amplitudes as shown in Fig.16c indicating a different level of ACC for slugs even in the same part.

The duration of the power pulse was ~ 20 msec; however, maximum temperature rise detected by IR camera happened long after (~0.5 sec) the power pulse was over, and the slug was cooling down. This is obviously due to the time necessary to heat up molding compound above the slug.

The characteristic time of heating that gives a time scale for thermal processes in the capacitor can be calculated as:

$$\theta = {L^2}/{\alpha}\ , \tag{4}$$

where L is the characteristic size of the element, and α is the thermal diffusivity, $\alpha = {k}/{(\rho c)}$, where k is the thermal conductivity, ρ is the specific density, and c is the specific heat capacity.

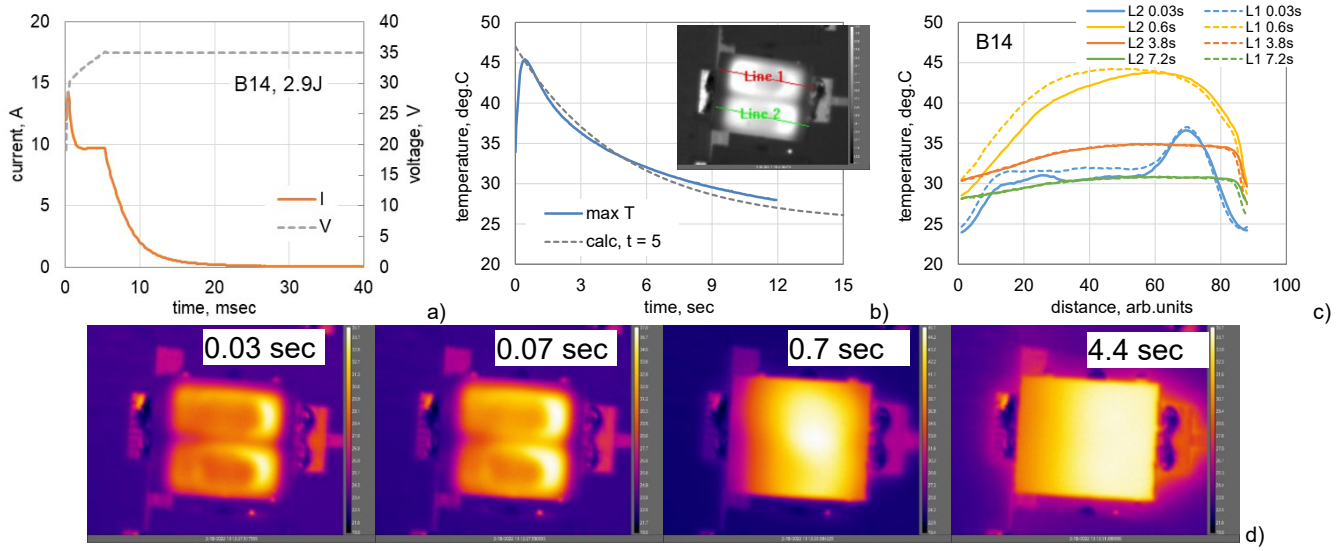

Fig.16. Voltage and current transients in a sample B14 of 100 µF 35 V capacitors (a), variations of maximum temperature with time (b) and temperature distributions along the lines 1 and 2 at the moments indicated in the legend (c). IR camera images taken at different moments after the pulse are displayed in Figures (d).

Thermal characteristics of the tantalum slug and molding compound (case) used for assessments of θ are shown in Table 2. Note, that considering that the porosity of the slug is ~50%, the values of the thermal conductivity and specific density were assumed to be 50% of the values for tantalum.

Assessments show that it takes approximately 100 msec to heat up the slug, whereas a few seconds are necessary to stabilize temperature of the case. This explains the lag between duration of the power pulse and time to maximum temperature measured on the surface of the case.

Table 2. Thermal characteristics of the tantalum slug and molding compound.

	Ta slug	case (MC)
k, W/(m×K)	29	0.9
c, J/(kg×K)	140	900
ρ, kg/m^3	8000	1100
L, mm	1.5	2
α, m^2/sec	2.6E-05	9.1E-07
θ, sec	0.09	4.4

For power pulses less than 100 msec, the heating of the slug occurs in adiabatic conditions, energy losses are negligibly small, and practically the whole energy that is dissipated in the capacitor during ACC, Q, is transferred to heat that increases temperature of the slug. In this case, the temperature rise of the slug can be calculated as:

$$\Delta T = {}^{Q}/_{(v \times \rho \times c)}, \quad (5)$$

where v is the volume of the slug. At the size of the slug 2.7×1.5×5.5 mm, $v = 22\ mm^3$.

Fig.17a shows variations of the experimental and calculated values of ΔT with the energy dissipated during PST for 5 samples of 100 µF 35 V capacitors. The temperature increases linearly with Q, and the range of variation is from 20 to 40 °C for experimental data and from 120 to 210 ºC for the data calculated per Eq.(5). Due to heat losses, the actual temperature of the slug should be somewhat less than the calculated value, but substantially greater than the temperature measured by the IR camera. Temperature rise during PST may create substantial thermo-mechanical stresses in the slug resulting in damage to the dielectric and failures similar to those shown in Fig.4.

Relaxation of temperature after PST pulses is due to cooling of capacitors soldered onto a PWB. Additional experiments show that the thermal resistance of the parts, R_θ is in the range from 20 to 40 K/W. The calculated thermal capacity of the part (two slugs and molding compound), C_θ is ~0.14 J/K. At these conditions, the characteristic time

of the temperature decay after power pulse is $\tau = R_\theta \times C_\theta = 2.8$ to 5.6 sec, which is close to the experimental data shown in Fig.17b.

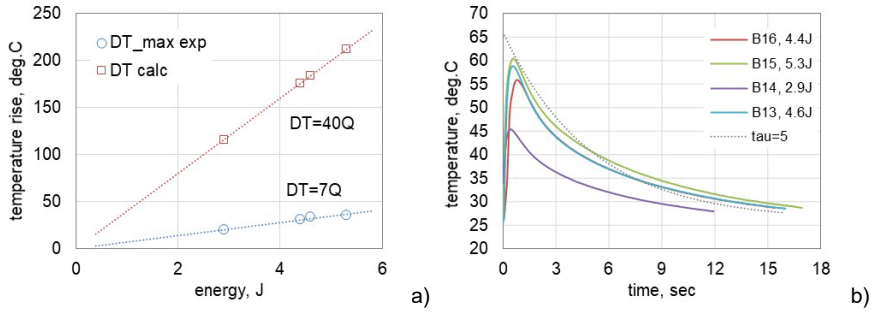

Fig.17. Variations of the experimental and calculated maximum temperatures with the energy of the pulse (a) and time dependence of temperature after application of power pulses for different samples (b). The legend indicates energy dissipated during PST.

V. DISCUSSION

Results of this study show that the level of ACC increases substantially when apparently dry capacitors (1 month storage at 85 °C) are baked for 1 week at 125 °C. On the other hand, capacitors dried out for one week at 125 °C can reduce ACC if baking continues at a lower temperature (85 °C). Also, baking at 150 °C for 3 hour is not as effective as 1 week at 125 °C. Considering that the level of moisture in polymers at a steady-state condition is proportional to relative humidity, we can obtain comparative assessments of the moisture content by analyzing variations of RH in a temperature chamber.

If RH and temperature at room conditions are $RH_{RC} = 40\%$ and $T_{RC} = 20$ °C, the absolute water pressure is $P_{RC} = 0.94$ kPa. Temperature variations of the saturated water pressure, $P_w(T)$, are shown in Fig.18a. Using these data, a relative humidity (%) in the chamber set to temperature T is:

$$RH_{ch}(T) = 100 \times {}^{P_w(T)}/_{P_{RC}} \tag{6}$$

Results of $RH_{ch}(T)$ calculations are shown in Fig.18b. As temperature increases from 85 °C to 125 °C, RH decreases almost 4 times. An increase from 125 °C to 150 °C reduces RH from 0.45% to 0.11%. At a solder reflow temperature of 235 °C for a Sn/Pb eutectic soldering process, $RH = 0.03\%$ and reduces to 0.019% at 260 °C for the lead-free solder process. The steady-state amount of moisture at these temperatures should change proportionally, and approximately 90 times reduction can be expected by increasing temperature from room temperature to 125 °C.

Stabilization of moisture content requires time that can be assessed for different temperatures assuming that the characteristic time for moisture desorption at 125 °C, $t_{bake} = 24$ hours:

$$t_{bake}(T) = t_{bake}(125) \times exp\left[\frac{E_a}{k}\left(\frac{1}{273+T} - \frac{1}{398}\right)\right], \tag{7}$$

where $E_a = 0.45$ eV [11] is the activation energy of the diffusion process.

Results of calculations of the characteristic times are shown in Fig. 18b. The bake time at 85 °C is ~ 100 hours, so one week at this temperature should stabilize the level of moisture. At 150 °C the characteristic time is 11 hr, so a 3-hour bake is not sufficient to reduce the level of moisture significantly. A substantial increase of ACC after one week at 125 °C for capacitors stabilized at 85 °C is likely due to almost four-time reduction of the moisture content. For sufficiently long storage times (weeks), a higher moisture content in parts dried at 125 °C will stabilize when the parts are stored at 85 °C. This explains the reduction of ACC levels observed experimentally.

There was no significant difference in ACC for parts after humidity chamber (85% RH) and after room condition (40% RH) storage. An increase of I_{10} after a 3 hr bake at 150 °C compared to room condition was relatively small. However, variations in capacitance during these tests were substantial. On the other hand, there were no significant changes in capacitance during different baking conditions that resulted in large variations of ACC. This means that the sensitivity of ACC to moisture is much greater, likely down to 0.1% RH, compared to the sensitivity of capacitance measurements that is expected at ~5 - 10% RH.

The required bake time to stabilize the level of moisture at 235 °C is around 1.4 hours and is far greater than the 20 sec required for the reflow process. This may explain why repeat reflow cycling increases ACC in the parts. An

increase in capacitance of initially dry parts after exposure to high temperatures (4 hr 175 °C and reflow simulation temperatures) indicates that moisture is not the only reason for capacitance changes. Delamination of PEDOT:PSS polymers that have a poor adhesion to tantalum pentoxide [16, 17] might be another reason for decreasing capacitance during high-temperature bakes.

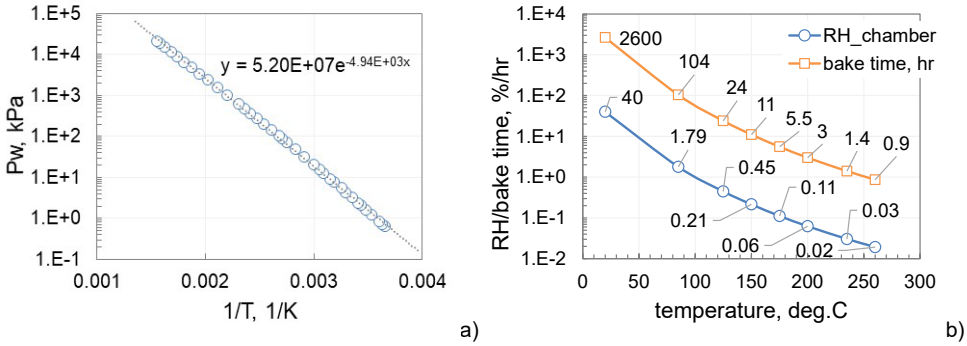

Fig.18. Temperature dependencies of the water saturation pressure (a) and the effective bake times (b). Figure (b) also shows variations of the relative humidity in a temperature chamber placed at room conditions, 40% RH, 20 °C.

Based on the moisture effect, no decrease in ACC after reflow soldering simulations of capacitors dried for 1 week at 125 °C can be expected. However, experimental data show the opposite. Also, ACC increases to a substantially greater degree after reflow soldering simulations of wet capacitors compared to dry parts. These data indicate that the amount of moisture may not be the only environmental factor affecting ACC.

Another possible reason for ACC variations may be structural changes in PEDOT:PSS polymers caused by exposure to high temperatures. The increase in crystallinity of PEDOT:PSS caused by heating to 150 – 170 °C in air and inert atmosphere was used in [18, 19] to explain variations of conductivity with temperature. Crystallization, as well as chemical decomposition of PEDOT:PSS occurs at high temperatures (~160 °C) with time, resulting in changes to optical characteristics and decreases of the Seebeck coefficient and electrical conductivity [20]. Due to high hygroscopicity of PEDOT:PSS systems, moisture absorption results in substantial swelling and morphological changes in the polymer [21]. Most likely, a moisture release during exposure to high temperatures forms different levels of crystallinity that depends on the initial moisture content and results in different post-soldering levels of ACC for dry and wet capacitors.

VI. CONCLUSION

1. The absence of a standardized test and a lack of manufacturing control results in large sample-to-sample and lot-to-lot variations of the ACC level in polymer tantalum capacitors. Issues with assessments of ACC are that the effect is divergent, changes with time due to moisture absorption, and charge accumulation during repeat measurements. ACC depends also on temperature and history of exposures to high temperatures.

2. Compared to the constant current and constant voltage ramp test methods, the suggested power surge testing (PST) results in maximum energy dissipation in capacitors. The thermal stresses associated with PST may result in sharp temperature increases of the slug up to 100 - 150 °C, may cause damage to the dielectric, and result in failures of capacitors. For this reason, PST in addition to the surge current testing, is recommended as a screening and lot acceptance procedure for polymer tantalum capacitors for space applications.

3. The level of ACC can be evaluated by currents measured at 10 msec, I_{10}, or energy dissipated in the process of current relaxation during PST, Q. The severity of ACC in different manufacturing lots of capacitors after bake at 125 °C for 24 hours can be characterized as high for parts with $I_{10} \geq 1$ A or $Q \geq 1$ J, as low for parts with $I_{10} < 0.1$ A or $Q < 0.1$ J, and as medium in other cases.

4. The significance of the ACC effect depends on the specific application conditions and may be negligible in at voltages below 0.5VR and relatively high temperatures (above ~65 °C). Lots with high ACC levels may require additional tests and analysis to assure reliable operation throughout mission life.

5. Anomalous transients are much more sensitive to the moisture content compared to capacitance variations. Even a relatively small amount of moisture, likely less than 10% of the amount absorbed at room conditions can suppress ACC substantially. However, exposure to high temperatures affects ACC even for dry capacitors. Reflow

soldering for initially wet capacitors can result in a much more significant increase in ACC compared to initially dry parts. This indicates that ACC is sensitive not only to the moisture content, but also to structural variations and the level of crystallization of PEDOT:PSS polymers.

6. At relatively low voltages corresponding to $I_{10} < 1$ A, the currents increase exponentially with the square root of voltage, which is consistent with the Schottky conduction mechanism. A decrease of currents during PST is likely due to increasing of the Schottky barrier with time. The relaxation of currents is not monotonic, and at high ACC levels *I-t* curves may have humps with amplitude and position that are dependent on temperature and applied voltage. Qualitatively, the humps can be explained by the space charge limited transient currents theory. However, voltage dependence of time to maximum and assessments for carriers' mobility are not consistent with literature. More analysis is necessary to fully understand mechanisms responsible for the ACC phenomena.

VII. ACKNOWLEDGMENT

The author is thankful to Susana Douglas, NASA Deputy EEE Parts Manager, and Chris Tiu, GSFC NEPP Task Monitor, for their review and discussion, and to Peter Majewicz, NEPP program manager, for support of this study. This work could not have been done without help from the GSFC PA Lab specialists and capacitor manufacturers who provided samples for this study.

REFERENCES

[1] A. Teverovsky, "Anomalous Transients in Chip Polymer Tantalum Capacitors," presented at the ESA 3rd International Symposium - Space Passive Component Days, Noordwijk, The Netherlands, 2018.
[2] Y. Freeman, G. F. Alapatt, W. R. Harrell, I. Luzinov, P. Lessner, and J. Qazi, "Anomalous Currents in Low Voltage Polymer Tantalum Capacitors," *Ecs Journal of Solid State Science and Technology,* vol. 2, pp. N197-N204, 2013
[3] A. Teverovsky, "Evaluation of 10V chip polymer tantalum capacitors for space applications," presented at the ESA 2nd International Symposium - Space Passive Component Days, Noordwijk, The Netherlands, 2016.
[4] J. Petržílek, M. Uher, and J. Navrátil, "Polymer tantalum capacitors with suppressed sensitivity to water content," presented at the 3rd Space Passive Component Days (SPCD), International Symposium, ESA/ESTEC, Noordwijk, The Netherlands, 2018.
[5] A. Tomás, C. Mota-Caetano, D. D. Lacombe, and L. Farhat, "Ta SMD capacitors with Polymer Counter Electrode for Space Applications," presented at the 3rd Space Passive Component Days (SPCD), International Symposium, ESA/ESTEC, Noordwijk, The Netherlands, 2018.
[6] M.Cozzolino, "Slection of polymer tantalum capacitors for class A space missions," in *Space Parts Working Group (SPWG-Aerospace)*, virtual, 2021, May 3-6.
[7] J. Voelm, "Exploration of Anomalous Charging Current (ACC) in Polymer Tantalum Capacitors," in *25th Components for Military and Space Electronics, CMSE'22*, virtual, 2022, April 25-29.
[8] P. L. Y. Freeman, I. Luzinovz, "Reliability and Failure Mode in Solid Tantalum Capacitors," *ESC J. Solid State Sci. Technol.,* vol. 10, 2021
[9] Y. Freeman and P. Lessner, "Evolution of Polymer Tantalum Capacitors," *APPLIED SCIENCES-BASEL,* vol. 11, JUN 2021
[10] A. Teverovsky, "Effect of Surge Current Testing on Reliability of Solid Tantalum Capacitors," in *The 28th Symposium for Passive Components, CARTS'08*, Newport Beach, CA, 2008, March 17-20, pp. 293-310.
[11] A. Teverovsky, "Effect of Moisture on AC Characteristics of Chip Polymer Tantalum Capacitors," *IEEE Transactions on Components, Packaging and Manufacturing Technology,* vol. 9, pp. 2282-2289, 2019
[12] A. Many and G. Rakavy, "Theory of Transient Space-Charge-Limited Currents in Solids in the Presence of Trapping," *Physical review,* vol. 126, pp. 1980-1988, 1962
[13] F. C. Aris and T. J. Lewis, "Steady and Transient Conduction Processes in Anodic Tantalum Oxide," *Journal of Physics D-Applied Physics,* vol. 6, pp. 1067-1083, 1973
[14] M.S. Mattsson, G. A. Niklasson, K. Forsgren, and A. Harsta, "A frequency response and transient current study of b-Ta2O5: Methods of estimating the dielectric constant, direct current conductivity, and ion mobility," *Journal of Applied Physics,* vol. 85, pp. 2185-2191, 1999
[15] A. Teverovsky, "Popcorning Failures in Polymer and MnO2 Tantalum Capacitors," *IEEE Transactions on Device and Materials Reliability,* vol. 21, pp. 33-40, 2021
[16] Z. Sita and M. Biler, "Ta capacitors with conductive polymer robust to lead free process," *AVX Technical information,* vol. S-TCCPR0M605-N, 2013
[17] Y. Freeman, I. Luzinov, R. Burtovyy, P. Lessner, W. Harrell, S. Chinnam*, et al.*, "Capacitance Stability in Polymer Tantalum Capacitors with PEDOT Counter Electrodes," vol. 6, pp. N104-N110, 2017
[18] E. Vitoratos, S. Sakkopoulos, N. Paliatsas, K. Emmanouil, and S. A. Choulis, "Conductivity Degradation Study of PEDOT: PSS Films under Heat Treatment in Helium and Atmospheric Air," *Open Journal of Organic Polymer Materials,* vol. 2, pp. 7-11, January 2012
[19] P. M. J. Huang, J. Wilson, A. Mello, J. Mello, D. Bradley, "Investigation of the Effects of Doping and Post-Deposition Treatments on the Conductivity, Morphology, and Work Function of Poly(3,4-ethylenedioxythiophene)/Poly(styrene sulfonate) Films," *Advanced functional materials,* vol. 15, pp. 290-296, 2005
[20] L. Stepien, A. Roch, R. Tkachov, B. Leupolt, L. Han, N. van Ngo*, et al.*, "Thermal operating window for PEDOT:PSS films and its related thermoelectric properties," *Synthetic Metals,* vol. 225, pp. 49-54, Mar 2017
[21] J. Zhou, D. H. Anjum, L. Chen, X. Z. Xu, I. A. Ventura, L. Jiang*, et al.*, "The temperature-dependent microstructure of PEDOT/PSS films: insights from morphological, mechanical and electrical analyses," *Journal of Materials Chemistry C,* vol. 2, pp. 9903-9910, 2014